RESEARCH MEMORANDUM

REDUCTIONS IN TEMPERATURE-RECOVERY FACTOR ASSOCIATED WITH PULSATING FLOWS GENERATED BY SPIKE-NOSED CYLINDERS AT A MACH NUMBER OF 3.50

By C. A. Hermach, Samuel Kraus, and John O. Reller, Jr.

Ames Aeronautical Laboratory
Moffett Field, Calif.

NATIONAL ADVISORY COMMITTEE FOR AERONAUTICS
WASHINGTON
March 4, 1957

NACA RM A56L05

[redacted]

NATIONAL ADVISORY COMMITTEE FOR AERONAUTICS

RESEARCH MEMORANDUM

REDUCTIONS IN TEMPERATURE-RECOVERY FACTOR ASSOCIATED WITH PULSATING FLOWS GENERATED BY SPIKE-NOSED CYLINDERS AT A MACH NUMBER OF 3.50

By C. A. Hermach, Samuel Kraus, and John O. Reller, Jr.

SUMMARY

An experimental investigation was made to determine the reductions in temperature-recovery factor associated with pulsating flows generated by spike-nosed cylinders. This investigation was conducted at zero angle of incidence, at a free-stream Mach number of 3.50, and at a free-stream Reynolds number, based on cylinder diameter, of 1.73 million.

The model consisted of a cylinder, 2 inches in diameter and 18 inches long, with a spike protruding from an annular chamber in the upstream end of the cylinder. The effects on recovery factor of variations in spike extension from 0 to 4 inches, in chamber depth from 0 to 0.9 inch, in spike diameter from 0.125 to 1.500 inches, and in spike vertex angle from 6° to 50° were studied.

It was found that pulsating flows, with resultant reductions in recovery factor, could be developed over the cylinder with a range of spike extensions for all the spikes and chamber depths tested. To achieve the maximum reductions in recovery factor on the cylinder, it was necessary to adjust each of the four geometric spike-nose parameters in conjunction with the others. For the range of spikes tested, the minimum temperature-recovery factors obtained varied from 0.66 to 0.74; the lower values were obtained with spikes of small diameter and vertex angle. The recovery factors were compared with the theoretical value of 0.849 for a laminar boundary layer and, for a given spike, approximately three fourths of the maximum reductions in cylinder recovery factor was attributed to adjustment of spike extension and the remainder to adjustment of chamber depth.

One of the best configurations tested, from the standpoint of reductions in recovery factor, consisted of a 0.250-inch-diameter, 15° vertex-angle spike at an extension of 1.85 inches and a chamber with a depth of

[redacted]

[redacted]

0.79 inch. With this configuration, the recovery factor was 0.660 at 3 inches and 0.722 at 16 inches downstream of the leading edge of the cylinder.

INTRODUCTION

Results of experiments with a novel type of unsteady boundary layer were reported in reference 1. In these experiments, the normal boundary layer on the surface of a truncated cone was periodically interrupted by large-scale vortices, generated by a spike which protruded from the upstream face of the cone. This unsteady flow was termed a "pulsating" or "boundary-layer-vortex" flow. Significant reductions in temperature-recovery factor on the surface bounded by such a flow were noted. It was indicated that the rate of heat transfer to the surface was also reduced. It appeared that these reductions were caused by the vortices which removed part of the heat added to the surface by the normal boundary layer.

In these initial experiments, however, no attempt was made to investigate systematically the effects of variations in spike-nose configuration on the resultant reductions in temperature-recovery factor. The present experimental investigation was initiated, therefore, to make such a systematic study. The model tested was a fineness-ratio-9 cylinder with a spike protruding from an annular chamber in the upstream face of the cylinder. The effects on cylinder recovery factor of variations in spike diameter, spike vertex angle, spike extension, and chamber depth were studied. Limited studies were also made of the recovery factors in the region of the nose and of the frequency with which the vortices were discharged over the model.

SYMBOLS

d_s spike diameter, in. (fig. 1)

N_{Str} Strouhal number, $\dfrac{\left(\begin{array}{c}\text{frequency of}\\ \text{flow disturbance}\end{array}\right)\left(\begin{array}{c}\text{characteristic}\\ \text{dimension}\end{array}\right)}{\text{free-stream velocity}}$

T_r recovery temperature, $^\circ R$

T_t stagnation temperature, $^\circ R$

T_∞ free-stream static temperature, $^\circ R$

X_c chamber depth, in. (fig. 1)

$\bar{X}_s$ spike extension, in. (fig. 1)

X_η, Y_η thermocouple position, in. (figs. 1 and 3)

α_s spike vertex angle, deg (fig. 1)

η_r temperature-recovery factor, $\frac{T_r - T_\infty}{T_t - T_\infty}$

EXPERIMENT

Apparatus and Tests

The experimental data from this investigation were obtained in the Ames 10- by 14-inch supersonic wind tunnel. This wind tunnel is of the continuous-flow type and operates with a nominal supply pressure of six atmospheres. A detailed description of the wind tunnel, of its associated equipment, and of the characteristics of the flow in the test region is presented in reference 2.

The tests were conducted at zero angle of incidence, at a free-stream Mach number of 3.50, and at a Reynolds number, based on free-stream conditions and cylinder diameter, of 1.73 million. The model was sting supported from the rear. The measured flow characteristics included recovery temperatures at various points on the model and the frequency of pulsation in the spike-nose region.

Models and Instrumentation

The model consisted of a fineness-ratio-9, thin-walled cylinder together with spikes, inserts, and insert liners, and was assembled as shown in figure 1. All parts of the model not otherwise specified were made of stainless steel.

The cylinder was 2 inches in diameter, 18 inches long, and had a wall thickness of 0.030 inch. The leading edge had an external bevel of 5° with a leading-edge radius of approximately 0.003 inch. Iron-constantan thermocouples were imbedded in the wall over the length of the cylinder, and were soldered on the external surface in the region of the leading edge. The cylinder was connected to the support sting through thin-walled spiders to minimize heat transfer from the sting to the cylinder. The spikes were supported in the cylinder by a combination of inserts and insert liners to accommodate various spike diameters. The points of support between the insert and the cylinder were separated by

[redacted]

[redacted]

a rubber "O" ring at the front and by nylon at the rear. Heat transfer between the insert and cylinder and air flow through the cylinder were thereby minimized.

The combination of insert and insert liner could be retracted inside the cylinder to form a chamber in the face of the cylinder. One insert contained a flush-mounted cell, sensitive to pressure variation, in the chamber face. The chamber depth could be varied from 0 to 0.9 inch during a test run. The spikes could be extended from 0 to 4 inches forward of the leading edge of the cylinder during a test run.

The spike configurations tested consisted of the following: twenty-four cone-cylinders with diameters ranging from 0.125 to 1.500 inches and with total vertex angles ranging from 6° to 50°; one cusp-cylinder; and one tangent-ogive cylinder. The latter two spikes formed a family with the 1.250-inch-diameter cone-cylinder spike. The dimensions of this family of spikes are indicated in figure 2. The diameters and vertex angles of all the spikes tested are given in table I.

A special version of the model was constructed which conformed in geometry with the forward section of the fineness-ratio-9 cylinder, as shown in figure 3. Thermocouples were imbedded in the chrome-molybdenum steel spike and in the micarta chamber face, and were soldered on the external surface of the chrome-molybdenum steel cylinder. The spike had a diameter of 0.250 inch and a total vertex angle of 15°. Spike extension and chamber depth could be adjusted between tests.

All model recovery temperatures, as well as the air-stream stagnation temperature, were measured on an indicating, self-balancing, precision potentiometer. The pressure cell used for the determination of the pulsation frequency was of the capacitance type. The output signal from the cell was amplified, passed through band-pass filters, and the resulting signal fed into an oscilloscope. The frequency of pulsation was then determined by the use of a precision frequency generator and the Lissajous figure technique.

Accuracy of Test Results

The errors which influenced the test results in general were as follows: Errors in spike extension and in chamber depth did not exceed ±0.01 inch. Mach number in the test region did not vary more than ±0.02 from the mean value. Reynolds number did not differ by more than ±30,000 from the mean value.

The temperatures measured in the spike-nose region were probably strongly influenced by the high rate of heat transfer through the model

materials which form this region. Therefore, the temperature-recovery factors presented for this region can be in substantial error, and the results can only be considered indicative of trends.

The maximum error in recovery factor on the cylinder (other than near the leading edge) occurred in the vicinity of the model-support spiders and was due to heat transfer from the support structure to the cylinder. The recovery factors presented for this region can be too high by as much as 0.035. However, in the locations where most of the data is compared (at X_η = 3 and 16 inches; see fig. 1), the limit of probable error in recovery factor was about ±0.005.

The error in measurement of the frequency of pulsation of pressure at the chamber face did not exceed ±50 cycles per second.

RESULTS AND DISCUSSION

The purpose of the present investigation was to determine the effects of variations in spike-nose geometry on the reductions in temperature-recovery factor associated with pulsating flows over a spike-nose cylinder. The majority of the results of this program, therefore, are presented to indicate the individual and over-all nature of these effects. In addition, limited results are presented on recovery factors in the spike-nose region and on the frequency with which vortices were discharged over the model.

Temperature-Recovery Factor

The temperature-recovery factors presented in this report are based on free-stream conditions. All the experimental data on recovery factor for the model are presented in tables I, II, and III. For discussion, a portion of the data is also presented in graphical form in figures 4 to 10.

Effects of spike extension.- The first test was conducted on the fineness-ratio-9 cylinder with the 0.250-inch-diameter, 15° vertex-angle spike to determine the effects of spike extension on recovery factors on the cylinder for zero chamber depth. The results are shown in figure 4 for two locations on the cylinder (X_η = 3 and 16 inches). With small spike extentions the flow was steady and the recovery factors were relatively high. As the spike was extended to penetrate the bow shock wave, pulsating flow commenced and the recovery factors decreased until the minimum recovery factors were reached. With further spike extension, pulsating flow stopped, a quasi-steady flow occurred, and the recovery factors rose sharply to values characteristic of normal boundary layers

and remained essentially constant with further spike extension. A detailed discussion of this pulsating flow phenomenon, with photographs of the various types of flow, can be found in reference 1. A considerable hysteresis effect was encountered in re-establishing pulsating flow once the spike had been extended past the point where the flow changed from pulsating to quasi-steady as also noted in reference 1. At a spike extension of 2.90 inches, the longest for which pulsating flow could be maintained, the lowest recovery factors were obtained. The recovery factor was 0.697 at 3 inches and 0.762 at 16 inches downstream of the leading edge of the cylinder. These recovery factors are about 18 and 10 percent lower, respectively, than the theoretical value of 0.849 for a laminar boundary layer.

Effects of chamber depth.- Next, the effect of introducing an additional variable, chamber depth, to this configuration was studied. It was found that the addition of a chamber of proper depth to the face of the model eliminated the hysteresis effect previously mentioned and reduced further the recovery factors on the cylinder (a similar effect was noted in ref. 1). Also, with the addition of the chamber, pulsating flow could be maintained with much greater spike extensions. It was found that the lowest temperature-recovery factors on the cylinder occurred at one spike extension for each chamber depth and that the value of spike extension changed as the chamber depth was changed. Both chamber depth and spike extension were, therefore, varied until the configuration was obtained which yielded the maximum reduction in recovery factor. It was found that two configurations of spike extension and chamber depth produced essentially the same minimum recovery factors. One configuration had a short spike extension and a deep chamber; the other had a comparatively long spike extension and shallow chamber.

The recovery factors along the cylinder for these configurations with a chamber are shown in figure 5 together with those for the best configuration without a chamber. Geometric sketches of these configurations are also shown. The effect of the chamber in reducing recovery factor is apparent. When compared with the theoretical value of recovery factor of 0.849 for a laminar boundary layer, approximately 20 percent of the over-all reduction in recovery factor at $X_\eta = 3$ inches and approximately 31 percent of the reduction at $X_\eta = 16$ inches can be attributed to the addition of the chamber. The relatively steep gradient in recovery factor in the region of $X_\eta = 0$ to $X_\eta = 2$ inches is characteristic of that encountered in the spike-nose region as will be discussed later. The slight peak in recovery factor in the region of $X_\eta = 9$ inches is probably due to heat transfer into the cylinder from the model structure as discussed under "Accuracy of Test Results."

Effects of variations in spike geometry.- The effects on recovery factor of variations in spike diameter and spike vertex angle were next determined. Again it was necessary to adjust both spike extension and chamber depth to obtain the maximum reduction in recovery factor for each

spike. It was found that for each spike the recovery factors were a minimum for two combinations of spike extension and chamber depth. For spike diameters of 0.375 inch and less, these two combinations have about the same minimum values and both are presented in table I. For spike diameters of 0.500 inch and greater, one combination of spike extension and chamber depth has substantially lower recovery factors than the other and only the values for this combination are presented in table I. The lowest minimum recovery factors for each spike are presented in figures 6 and 7, and the corresponding spike extension and chamber depth for each spike are presented in table I.

The recovery factors at X_η = 3 and 16 inches are presented because the values at X_η = 3 inches are indicative of the greatest reductions obtainable on the cylinder, and those at X_η = 16 inches are indicative of the degree with which these reductions extend along the cylinder. The values of recovery factor at these two stations are therefore used to illustrate the variations of recovery factor with spike diameter and with spike vertex angle.

The variation of recovery factor with spike diameter for various spike vertex angles is shown in figure 6. It will be noted that the recovery factors are lowest for a spike diameter of 0.250 inch at both stations. Also, the variation of recovery factor with spike diameter is essentially the same at both stations. It is apparent that, even with the largest spike diameters tested, there is a significant reduction in the recovery factors on the cylinder when compared with a theoretical laminar value of 0.849. The widest range of spike diameters was tested with the 30° vertex angle. For this group of spikes, the maximum variation in recovery factor with spike diameter was about 12 percent at X_η = 3 inches and about 7 percent at X_η = 16 inches.

The variation of recovery factor with spike vertex angle is more clearly illustrated in figure 7. Variation of spike vertex angle had little effect on recovery factor in the range of spike vertex angles tested. For the results shown in figure 7, for the families of spikes with a constant diameter, this variation was less than 4 percent at both X_η = 3 and 16 inches.

In review of figures 6 and 7, then, the maximum variation in recovery factor due to variation of spike diameter and vertex angle occurs between the 1.500-inch-diameter, 30° vertex-angle spike and the 0.250-inch-diameter, 20° vertex-angle spike. The recovery factors at X_η = 3 inches for these two spikes are 0.744 and 0.652, respectively. When compared with the theoretical laminar recovery factor of 0.849, it can be seen that the smaller spike was approximately twice as effective in reducing recovery factor.

A limited study of the effect of spike forebody shape on the recovery factors on the cylinder was next made utilizing the spikes illustrated in

[redacted]

figure 2. The results of this study are presented in figure 8. It can be seen that the conical-nosed and ogival-nosed spikes produced essentially the same variation of recovery factor along the cylinder, and that the recovery factors for the cusp-nosed spike were substantially lower than for the other two spikes over most of the cylinder. (The discontinuity of the curves representing data from the imbedded and external thermocouples is probably due to the steep temperature gradients which existed through the cylinder in the nose region, coupled with the slightly different methods of attachment of the imbedded and external thermocouples to the cylinder.) It is conjectured that the lower recovery factors obtained with the cusp-nosed spike result from the effectively smaller diameter of the spike as illustrated by the geometrically scaled sketches of these configurations in figure 8. If the effective spike diameter forward of the lip of the cylinder is the important parameter, it is apparent from the results of figure 6 that the cusp-nosed spike should produce the lower recovery factors.

The above conjecture is substantiated to some extent by the comparison made in figure 9. In this figure, the variations in minimum recovery factors on the cylinder for the cusp-nosed spike configuration are compared with those for the 0.250-inch-diameter, 15° vertex-angle spike configuration. It will be noted that downstream of $X_\eta = 9$ inches the recovery factors are the same. Upstream of this point the higher recovery factors associated with the cusp-nosed spike configuration may be due to the shape of the chamber. The wedge-shaped region between the spike and the insert liner can, in pulsating flow, produce local air temperatures greater than those associated with a flat chamber face (see Sprenger, ref. 3) with a resultant increase in heat transfer from this region to the cylinder.

Configuration for lowest cylinder recovery factors.- From the results of figures 6, 7, and 9, it can be seen that the minimum recovery factors on the cylinder were obtained with the 0.250-inch-diameter spike and with a spike vertex angle between 15° and 20°. As an illustration of the maximum reductions in recovery factor obtained on the cylinder, then, the results from the model with the 0.250-inch-diameter, 15° vertex-angle spike will be used. For this spike, with a spike extension of 1.85 inches and a chamber depth of 0.79 inch, the recovery factor was 0.660 at $X_\eta = 3$ inches and 0.722 at $X_\eta = 16$ inches. These values are, respectively, approximately 22 and 15 percent below a theoretical value of 0.849 for a laminar boundary layer-flow, and approximately 26 and 20 percent below a theoretical value of 0.897 for a turbulent boundary layer.

Recovery factors in the spike-nose region.- Since the model with the 0.250-inch-diameter, 15° vertex-angle spike had, in general, the lowest recovery factors on the cylinder, this spike-nose configuration was chosen for the determination of the corresponding recovery factors in the spike-nose region. The model sketched in figure 3 was used for this investigation. The spike extensions and chamber depths tested were the

same as for the two configurations of figure 5. Recovery factors were measured on the spike, the chamber face, and the cylinder. The results of these tests are shown in figure 10 along with superimposed sketches of the model for identification of the thermocouple locations.

It will be noted that the recovery factors vary over a wide range in the spike-nose region. It is apparent that, due to heat transfer through the model materials, the recovery factors shown can differ greatly from the true values. Some of the trends indicated by these results can, however, be discussed. The recovery factors are highest on the face of the chamber; in fact, most of the recovery factors are greater than 1.0 or, in other words, the temperatures measured on the chamber face are higher than the stagnation temperature of the air stream. These results may be related to the results of Sprenger (ref. 3) on resonating flow in tubes. The recovery factors on the spike could probably be, on the average, substantially lower if heat were not being transferred to the spike from the chamber. It is significant that, despite this heat flow, some of the recovery factors on the spike for the configuration of figure 10(b) reach values much lower than the theoretical value for a laminar boundary layer. It is conjectured that these low spike recovery factors are associated with the periodic shedding of the vortices formed in this region, as discussed in reference 1. It is also apparent that the measured recovery factors on the cylinder in this region can be strongly influenced by heat transfer from the chamber. (Note the similar precipitous drop in recovery factor in this region in figure 5.)

Frequency of Pulsation

Since pulsating flow is initiated by the cyclic generation of vortices in the spike-nose region of a model, it was considered to be of interest to determine the rate at which these pulsations occurred. The results of these tests will be presented in terms of both measured frequency and Strouhal number. The dimension in Strouhal number found to be most characteristic for the present tests is the sum of spike extension and chamber depth.

These tests were conducted with the model shown in figure 1. For most of the tests, the 0.250-inch-diameter, 15° vertex-angle spike and a constant chamber depth of 0.48 inch were utilized. With this spike-nose configuration, the effects of variations in spike extension on pulsation frequency were studied. Limited tests were also made with two other configurations: one consisted of the 0.250-inch-diameter, 15° vertex-angle spike with a spike extension of 1.85 inches and a chamber depth of 0.79 inch, and the other consisted of the 1-inch-diameter, 15° vertex-angle spike with a spike extension of 3.10 inches and a chamber depth of 0.37 inch.

[redacted]

The results of these tests are shown in figure 11, where both frequency and Strouhal number are presented as functions of spike extension. For the test with variable spike extension, the frequency decreased from 2000 to 1420 cycles per second as the spike was extended from 1.75 to 4.13 inches. For the other two configurations, discrete test points were obtained which did not correlate with the above results. In fact, at a spike extension of 1.85 inches, a pronounced effect of chamber depth on frequency can be seen for the model with the 0.250-inch-diameter spike.

When frequency is presented in terms of Strouhal number, a dimensionless correlation can be obtained at least for the spike-nose configurations tested. It should be noted that this correlation requires that Strouhal number be presented as a function of spike extension even though Strouhal number itself contains a dimension of spike extension plus chamber depth. The variation of Strouhal number with spike extension is probably caused by the change in Reynolds number, based on spike extension. An influence of Reynolds number on Strouhal number is pointed out in reference 4.

CONCLUSIONS

Within the conditions of the present investigation, the following conclusions are drawn:

1. Pulsating flow with associated reductions in temperature-recovery factors is developed over the cylinder with a range of spike extensions for all the spikes and chamber depths tested. The reductions in recovery factor which result, however, are maximized only at discrete combinations of spike extension and chamber depth for each spike. The four variations in spike-nose configuration tested (i.e., spike diameter, spike vertex angle, spike extension, and chamber depth) are interdependent in their effects on recovery factor and each must be adjusted in conjunction with the others to achieve the maximum reductions in recovery factor.

2. For the range of spikes tested, the minimum temperature-recovery factors obtained vary from 0.66 to 0.74; the lower values are obtained with spikes of small diameter and vertex angle. The variations in recovery factor due to change in spike diameter are, in general, about twice as large as variations due to change in vertex angle.

3. For a given spike, approximately three fourths of the maximum reductions in cylinder recovery factor is attributed to adjustment of spike extension and the remainder to adjustment of chamber depth, when compared with a theoretical value of recovery factor of 0.849 for a laminar boundary layer.

4. One of the best configurations, in terms of maximum reduction of recovery factor on the cylinder, consists of a 0.250-inch-diameter, 15° vertex-angle spike at an extension of 1.85 inches and a chamber which is 0.79 inch deep. With this configuration the recovery factor is 0.660 at 3 inches and 0.722 at 16 inches downstream of the leading edge of the cylinder. These values are 22 and 15 percent lower, respectively, than the theoretical laminar recovery factor of 0.849. In the spike-nose region of this configuration, the recovery factors are relatively high. The highest recovery factors occur on the face of the annular chamber and are slightly greater than 1.0.

Ames Aeronautical Laboratory
National Advisory Committee for Aeronautics
Moffett Field, Calif., Dec. 5, 1956

REFERENCES

1. Eggers, A. J., Jr., and Hermach, C. A.: Initial Experiments on the Aerodynamic Cooling Associated With Large-Scale Vortical Motions in Supersonic Flow. NACA RM A54L13, 1955.

2. Eggers, A. J., Jr., and Nothwang, George J.: The Ames 10- By 14-Inch Supersonic Wind Tunnel. NACA TN 3095, 1954.

3. Sprenger, Herbert: Über thermische Effekte in Resonanzrohren. Institut Für Aerodynamik, Eidgenössichen Technischen Hochschule, Zürich, Nr. 21., 1954. (English Summary)

4. Rayleigh, J.: Theory of Sound. Dover Pub., 1945.

[redacted]

TABLE I.- MINIMUM RECOVERY FACTORS ON CYLINDER FOR EACH SPIKE

Spike diameter, d_s, in.	Spike total vertex angle, α_s, deg	Spike extension Y_s, in.	Chamber depth, X_c, in.	Temperature-recovery factor, η_r, at																				
				External thermocouple position, X_η, in.						Embedded thermocouple position, X_η, in.														
				1/4	1/2	3/4	1	1-1/2	2	2	3	4	5	6	7	8	9	10	11	12	13	14	15	16
0.125	15	2.19	0.83	0.894	0.895	0.907	0.805	0.745	0.716	—	0.659	0.670	0.687	0.703	0.716	0.714	0.723	0.708	0.706	0.709	0.712	0.715	0.720	0.727
.250	10	1.94	.76	.864	.908	.908	.773	.712	.681	—	.664	.667	.687	.693	.701	.709	.723	.709	.706	.708	.711	.715	.720	.727
.250	10	4.06	.51	.826	.815	.770	.681	.666	.655	—	.636	.639	.691	.678	.704	.714	.729	.716	.714	.718	.719	.722	.726	.729
.250	15	1.85	.79	.851	.887	.896	.782	.717	.684	—	.660	.651	.672	.684	.698	.700	.705	.697	.698	.701	.705	.710	.715	.722
.250	15	3.86	.48	.827	.826	.786	.689	.668	.655	—	.649	.652	.687	.687	.696	.707	.721	.707	.706	.709	.711	.715	.719	.724
.250	20	1.84	.74	.845	.885	.892	.786	.721	.688	—	.664	.669	.698	.702	.703	.713	.726	.710	.709	.711	.714	.718	.723	.730
.250	20	3.58	.53	.835	.833	.794	.693	.671	.659	—	.632	.662	.682	.683	.696	.708	.723	.707	.707	.709	.711	.715	.719	.725
.250	30	1.54	.80	.840	.877	.887	.780	.722	.693	—	.669	.671	.683	.699	.707	.712	.719	.712	.712	.715	.719	.724	.728	.734
.250	30	3.25	.49	.847	.829	.780	.690	.672	.661	—	.637	.667	.683	.685	.696	.706	.717	.707	.708	.712	.715	.719	.724	.729
.375	6	1.94	.75	.855	.902	.909	.778	.720	.690	—	.677	.692	.752	.733	.730	.736	.744	.725	.721	.722	.724	.728	.733	.739
.375	6	3.25	.43	.888	.839	.793	.698	.683	.671	—	.677	.700	.737	.724	.730	.738	.748	.733	.731	.732	.733	.736	.739	.743
.375	10	1.91	.69	.868	.912	.916	.760	.719	.688	—	.671	.677	.707	.712	.714	.724	.735	.718	.716	.717	.719	.724	.728	.735
.375	10	4.00	.37	.840	.807	.764	.682	.672	.664	—	.687	.689	.714	.717	.724	.733	.746	.731	.730	.733	.734	.737	.740	.749
.375	15	1.88	.74	.864	.904	.915	.792	.726	.692	—	.676	.681	.709	.717	.721	.729	.739	.723	.720	.722	.725	.729	.734	.741
.375	15	4.06	.44	.822	.819	.776	.687	.670	.663	—	.661	.674	.696	.703	.712	.723	.738	.721	.719	.721	.722	.725	.729	.733
.375	20	1.82	.82	.845	.882	.893	.804	.735	.701	—	.682	.684	.710	.719	.721	.735	.743	.726	.724	.726	.729	.733	.737	.744
.375	20	4.06	.49	.819	.826	.789	.684	.664	.654	—	.671	.667	.690	.699	.706	.716	.730	.713	.712	.714	.717	.720	.724	.730
.375	30	1.72	.81	.854	.895	.907	.805	.745	.716	—	.699	.704	.729	.737	.739	.752	.757	.742	.739	.740	.743	.747	.751	.756
.375	30	3.00	.58	.861	.865	.822	.712	.684	.668	—	.661	.668	.691	.703	.714	.725	.737	.717	.716	.717	.720	.724	.728	.735
.500	10	3.40	.49	.889	.892	.812	.711	.684	.668	0.658	.661	.676	.710	.697	.710	.718	.723	.713	.717	.720	.723	.728	.733	.737
.500	15	4.00	.60	.819	.838	.815	.714	.690	.674	.665	.667	.675	.688	.701	.712	.719	.725	.715	.718	.722	.725	.729	.733	.737
.500	20	4.00	.60	.829	.840	.816	.713	.688	—	.670	.671	.677	.688	.700	.709	.718	.712	.712	.716	.720	.723	.728	.732	.737
.500	30	3.52	.77	.833	.910	.917	.799	.736	.703	.700	.686	.687	.696	.709	.720	.723	.721	.722	.726	.730	.734	.738	.743	.750
.750	30	2.34	.33	.866	.780	.754	.692	.694	.686	.679	.690	.717	.729	.725	.736	.745	.744	.745	.749	.753	.756	.760	.766	.770
1.000	15	3.52	.55	.867	.874	.841	.731	.691	.691	.702	.689	.694	.703	.713	.731	.737	.732	.732	.735	.739	.741	.744	.748	.752
1.000	20	3.05	.44	.866	.827	.790	.702	.680	.680	.714	.691	.698	.714	.728	.760	.764	.752	.746	.749	.753	.754	.758	.762	.767
1.000	30	2.84	.29	.821	.764	.738	.683	.677	.678	.699	.684	.693	.709	.719	.735	.739	.737	.739	.743	.748	.750	.754	.759	.764
1.000	40	1.86	.53	.877	.933	.924	.792	.727	.708	.719	.702	.716	.749	.738	.752	.755	.750	.749	.751	.754	.757	.761	.765	.770
1.000	50	1.47	.42	.816	.850	.834	.735	.703	.703	.712	.703	.725	.757	.741	.751	.755	.753	.753	.756	.759	.761	.765	.770	.714
1.125	19	3.24	.41	.849	.788	.753	.682	.676	.670	.714	.683	.691	.700	.708	.721	.730	.730	.732	.736	.741	.743	.748	.753	.757
1.250	cusp	2.02	.56	.916	.929	.931	.790	.730	.706	.811	.699	.684	.687	.697	.701	.708	.701	.699	.700	.703	.706	.711	.716	.722
1.250	22	3.08	.39	.876	.817	.776	.708	.696	.690	.686	.696	.702	.712	.721	.735	.742	.740	.742	.746	.750	.754	.758	.762	.766
1.250	30	2.52	.39	.855	.796	.766	.703	.692	.687	.687	.697	.704	.713	.717	.727	.739	.739	.741	.746	.751	.753	.758	.762	.767
1.250	ogive	2.59	.41	.870	.818	.779	.713	.704	.700	.738	.707	.709	.719	.732	.740	.746	.743	.745	.750	.755	.757	.762	.767	.771
1.500	30	2.12	.57	.971	.969	.932	.810	.762	.745	.742	.744	.745	.751	.753	.758	.765	.767	.768	.772	.775	.777	.781	.784	.788

TABLE II.- VARIATION WITH SPIKE POSITION OF RECOVERY FACTOR ON CYLINDER FOR ZERO CHAMBER DEPTH; d_s = 0.250 IN., α_s = 15°

(a) Extension of spike				(b) Retraction of spike			
Spike extension, $\bar{X}_s$, in.	Temperature-recovery factor, η_r, at imbedded thermocouple location, X_η, in.			Spike extension, $\bar{X}_s$, in.	Temperature-recovery factor, η_r, at imbedded thermocouple location, X_η, in.		
	3	10	16		3	10	16
0.30	0.909	0.901	0.903	4.00	0.842	0.862	0.862
.40	.909	.902	.904	3.60	.839	.861	.863
.70	.888	.892	.894	3.20	.835	.859	.862
.90	.836	.862	.863	3.00	.838	.861	.863
1.00	.810	.846	.849	2.90	.841	.868	.866
1.20	.759	.811	.818	2.80	.843	.869	.868
1.40	.737	.794	.804	2.70	.840	.867	.867
1.60	.733	.783	.793	2.60	.837	.865	.865
1.80	.731	.781	.792	2.50	.838	.865	.866
2.00	.718	.771	.783	2.40	.837	.865	.866
2.10	.713	.767	.779	2.30	.837	.865	.867
2.20	.711	.765	.778	2.20	.832	.862	.865
2.30	.709	.764	.776	2.10	.828	.860	.863
2.40	.706	.762	.773	2.00	.719	.775	.784
2.50	.705	.759	.770	1.90	.724	.777	.788
2.60	.704	.756	.767	1.80	.731	.781	.792
2.70	.702	.755	.765	1.70	.735	.783	.794
2.80	.700	.754	.764	1.60	.733	.782	.792
2.90	.697	.751	.762	1.50	.731	.783	.794
3.00	.838	.852	.859	1.40	.735	.789	.801
3.10	.835	.854	.860	1.30	.742	.794	.806
3.20	.834	.855	.861	1.20	.759	.804	.814
3.40	.837	.858	.861	1.10	.784	.822	.830
3.60	.838	.859	.862	1.00	.809	.838	.844
3.80	.845	.863	.865	.90	.835	.854	.859
4.00	.842	.861	.862	.80	.865	.873	.878
4.17	.840	.859	.860	.70	.887	.886	.891
				.60	.908	.899	.902
				.50	.909	.900	.903
				.40	.909	.901	.903

TABLE III.- RECOVERY FACTOR IN THE NOSE REGION OF THE MODEL WITH THE 0.250 IN., 15° VERTEX ANGLE SPIKE

Spike extension, $\bar{X}_s$, in.	Chamber depth, X_c, in.	Temperature-recovery factor, η_r					
		Spike		Cylinder		Chamber face	
		X_η in.	η_r	X_η in.	η_r	Y_η in.	η_r
1.85	0.79	-1.29	0.896	0.25	0.838	0.25	1.027
		-.04	.936	.50	.858	.44	1.046
		.71	1.001	.75	.846	.62	1.081
				1.00	.817	.81	1.083
				1.50	.783		
3.86	.48	-3.30	.836	.25	.814	.25	.907
		-2.05	.781	.50	.825	.44	.937
		-1.30	.776	.75	.763	.62	1.019
		-.58	.797	1.00	.742	.81	1.039
		-.05	.861	1.50	.725		
		.39	.900				

[redacted]

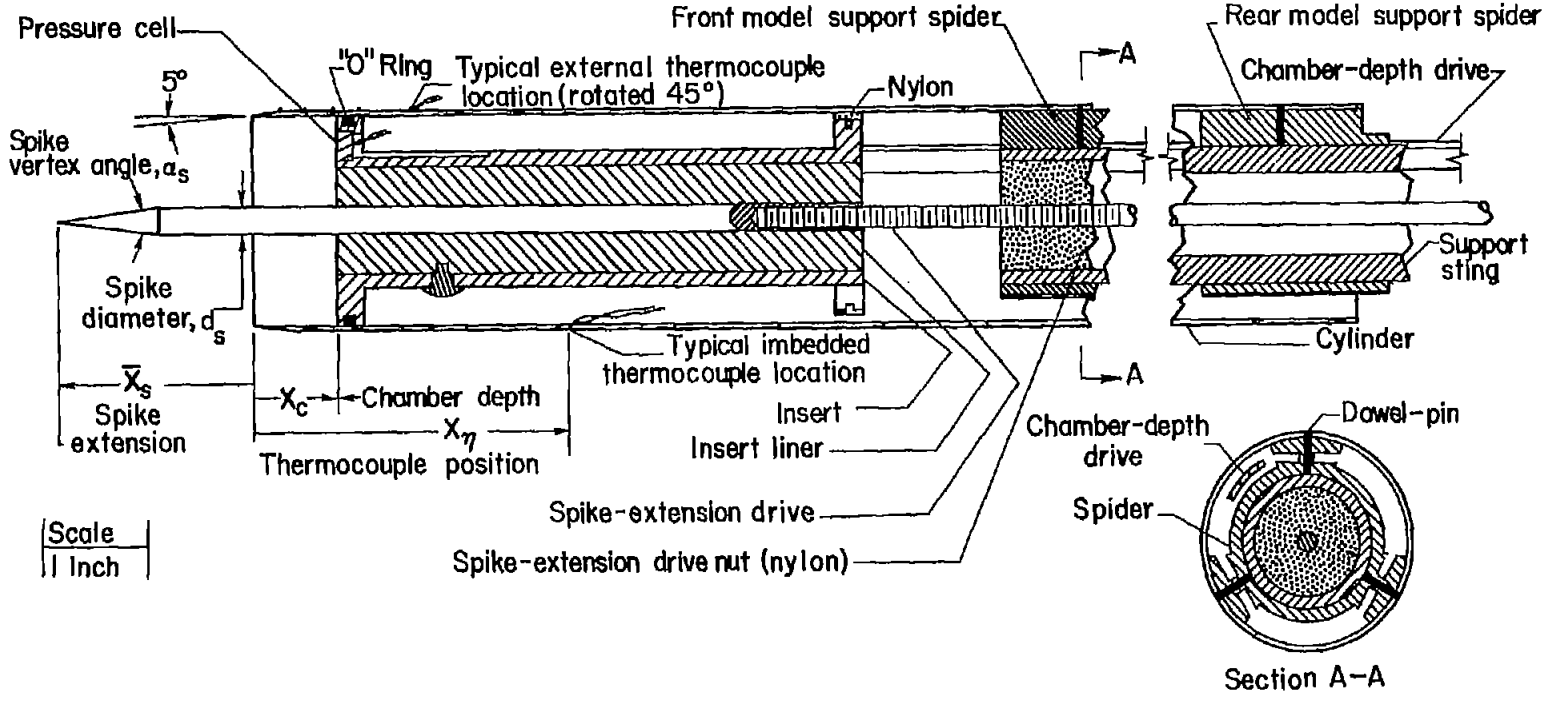

Figure 1.- Typical model installation for determination of recovery factors on the cylinder.

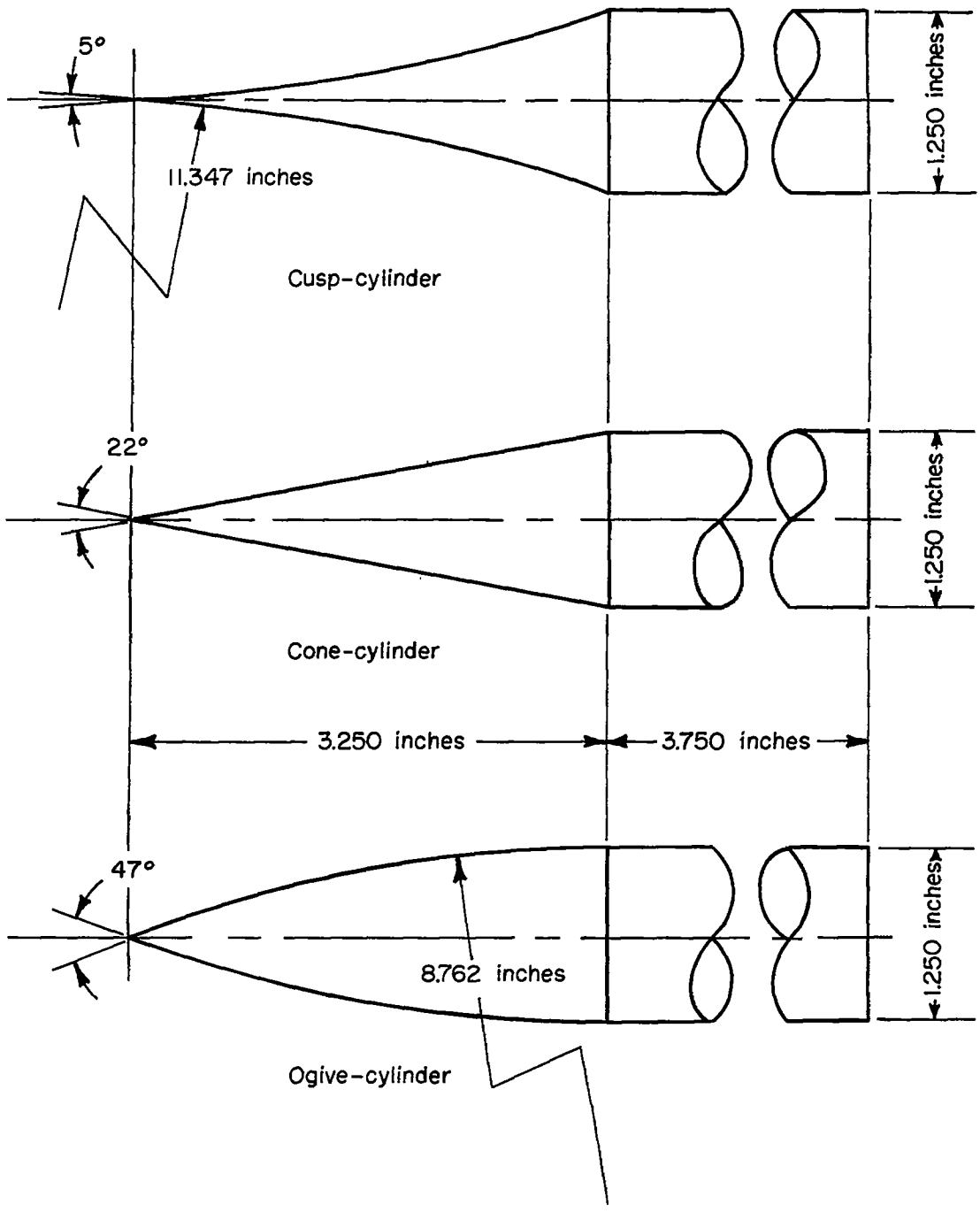

Figure 2.- The cusp-, cone-, and ogive-cylinder family of spikes.

[redacted]

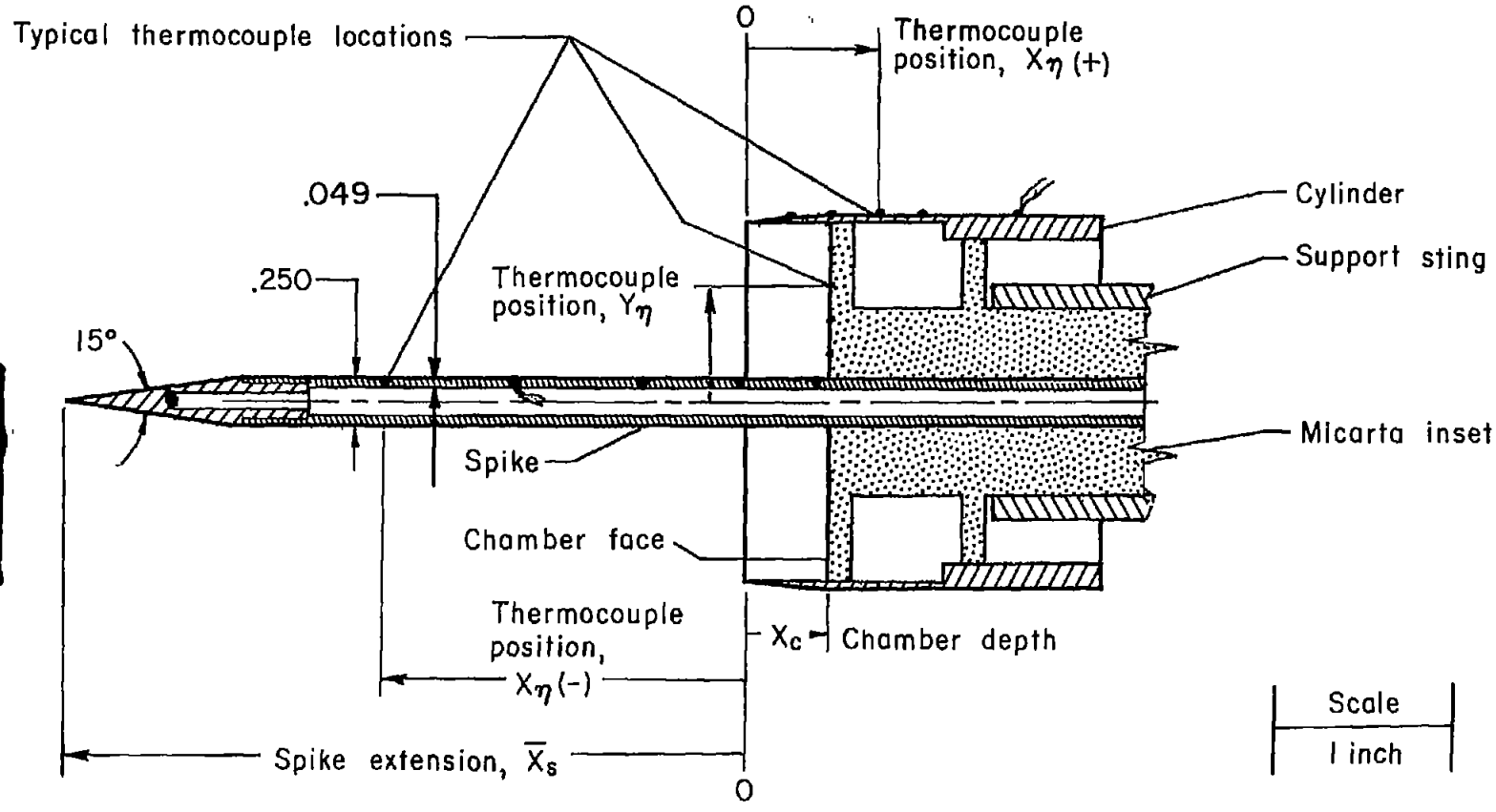

Figure 3.- Typical model installation for determination of recovery factors in the spike-nose region.

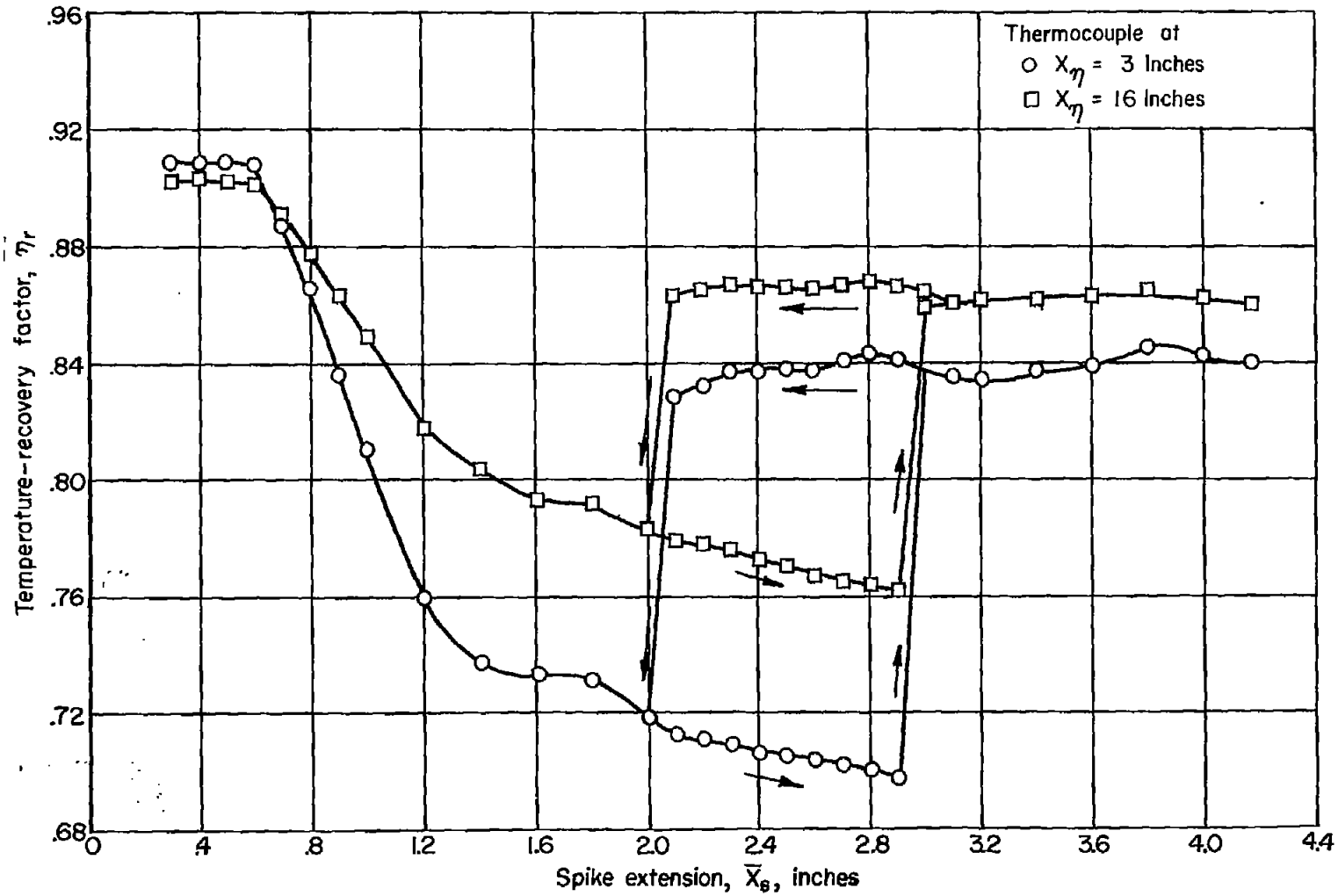

Figure 4.- Variation of recovery factor with spike extension; d_s = 0.250 inch, α_s = 15°, X_c = 0 inch.

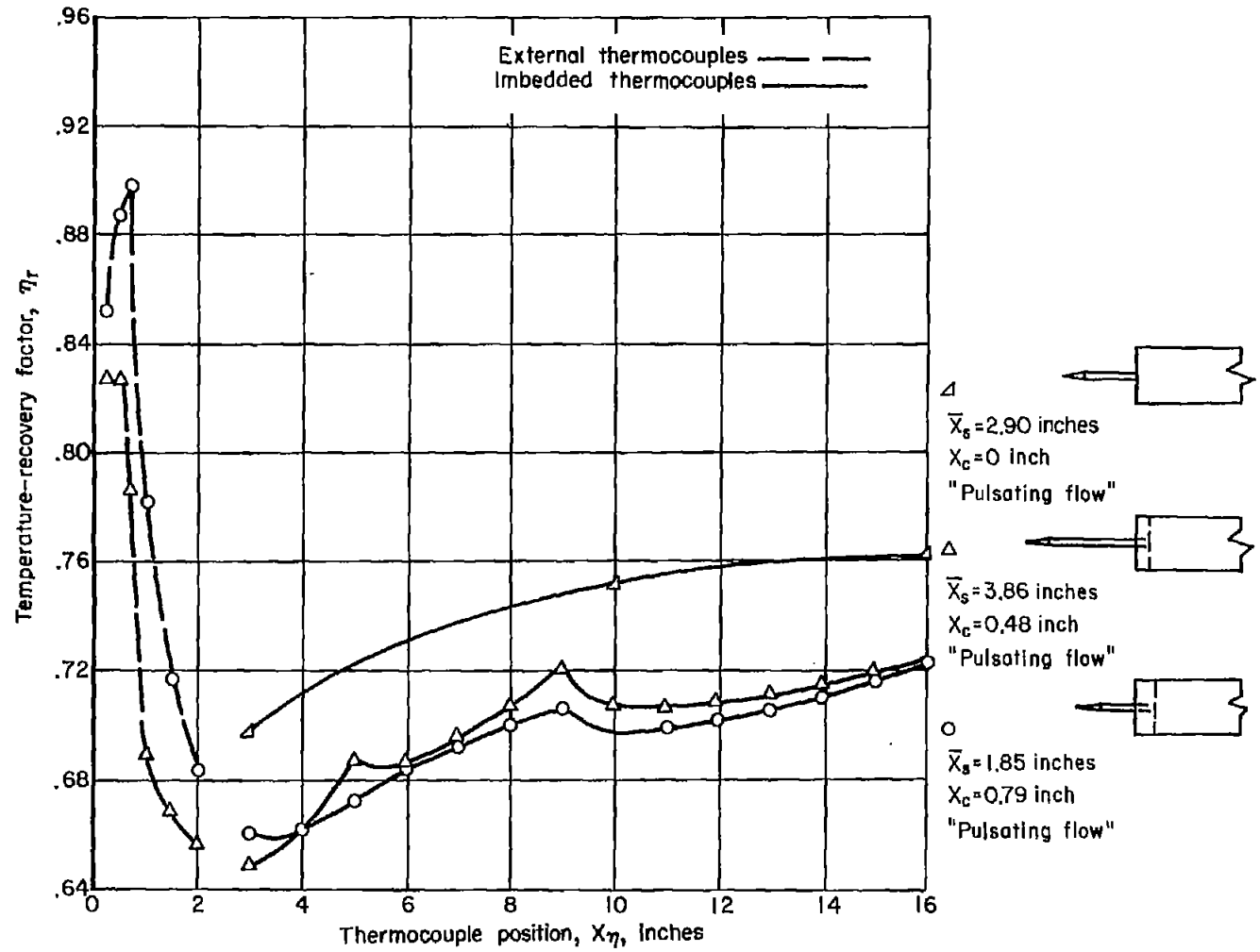

Figure 5.- Variation of recovery factor along the cylinder for optimum spike extension for several chamber depths; d_s = 0.250 inch, α_s = 15°.

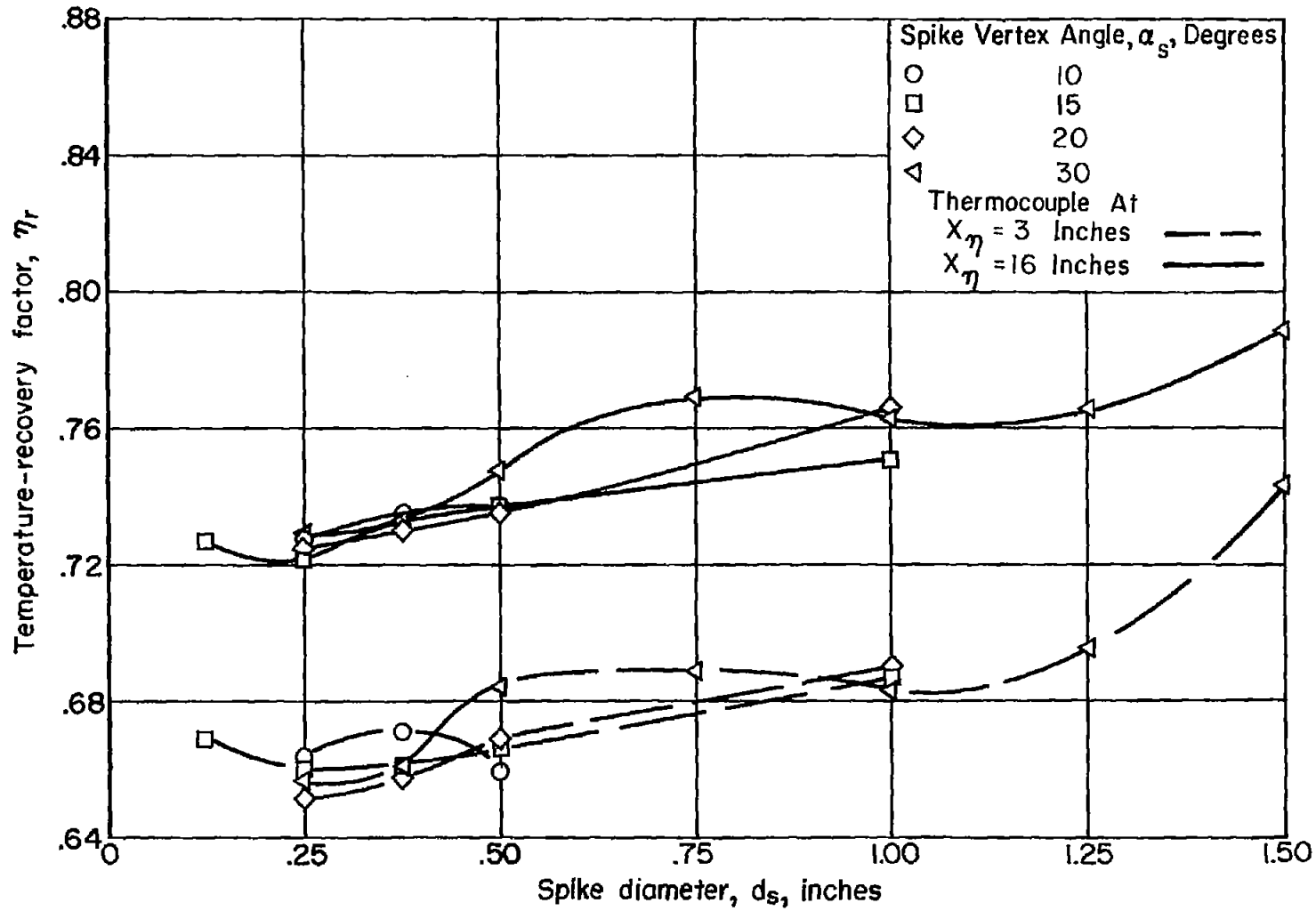

Figure 6.- Variation of minimum recovery factor with spike diameter for various spike vertex angles.

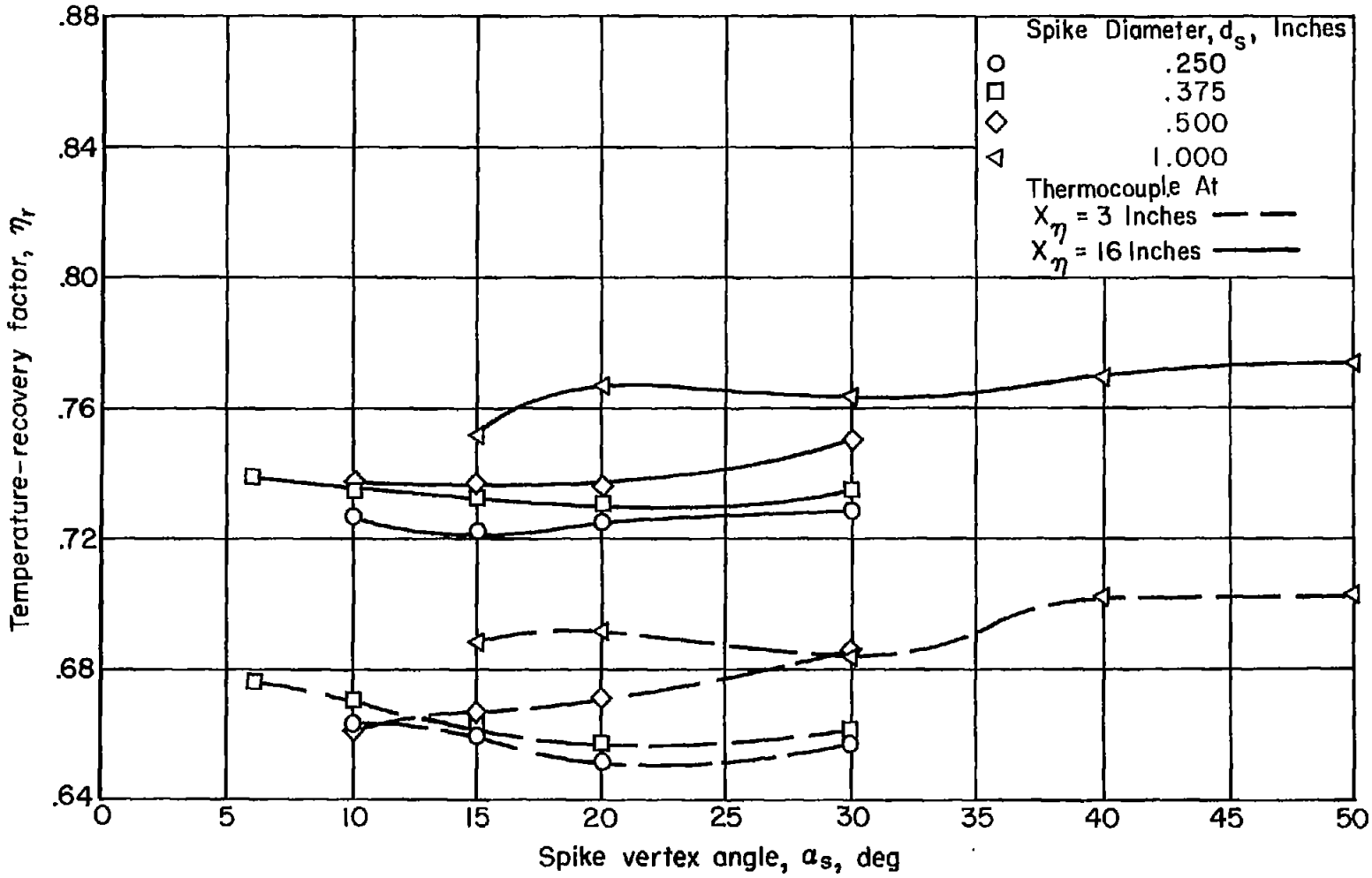

Figure 7.- Variation of minimum recovery factor with spike vertex angle for various spike diameters.

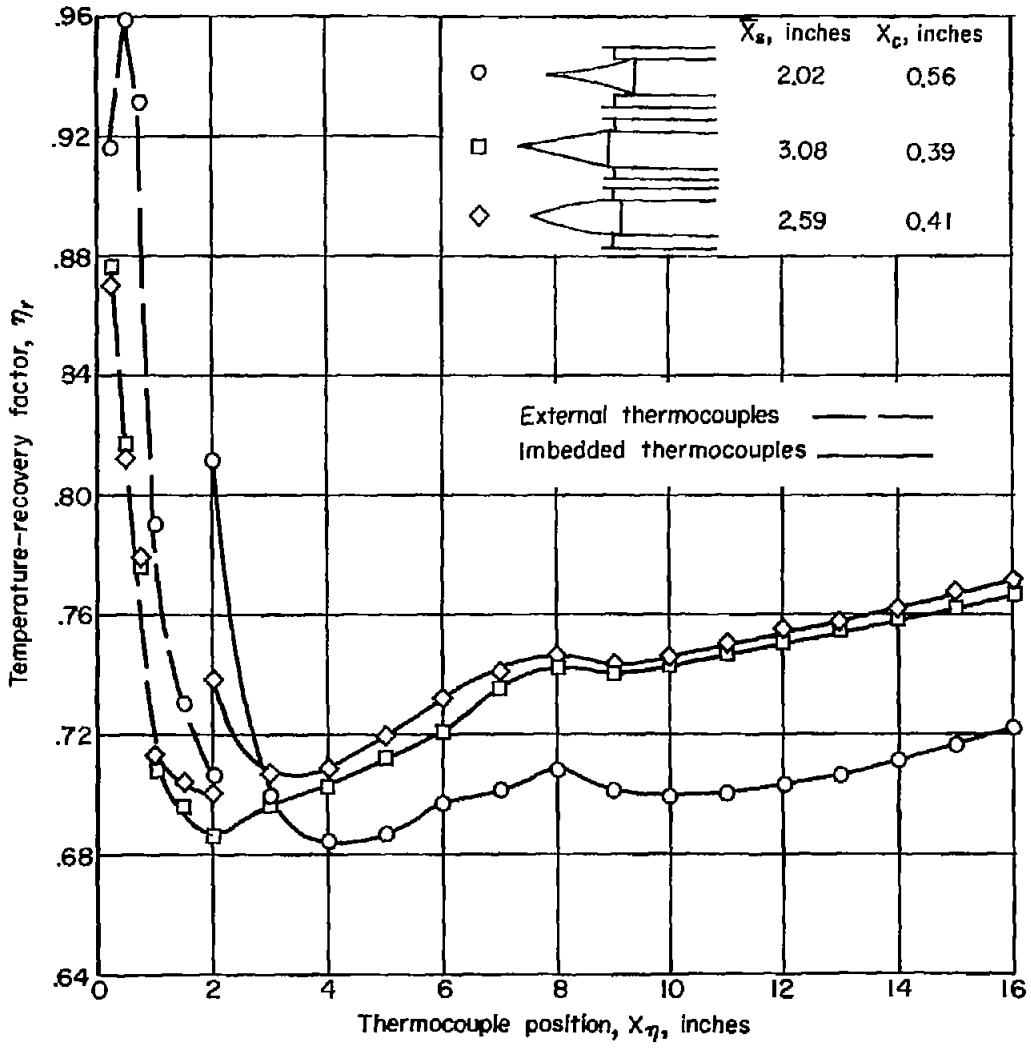

Figure 8.- Effect of spike forebody shape on recovery factor along the cylinder; d_s = 1.250 inches.

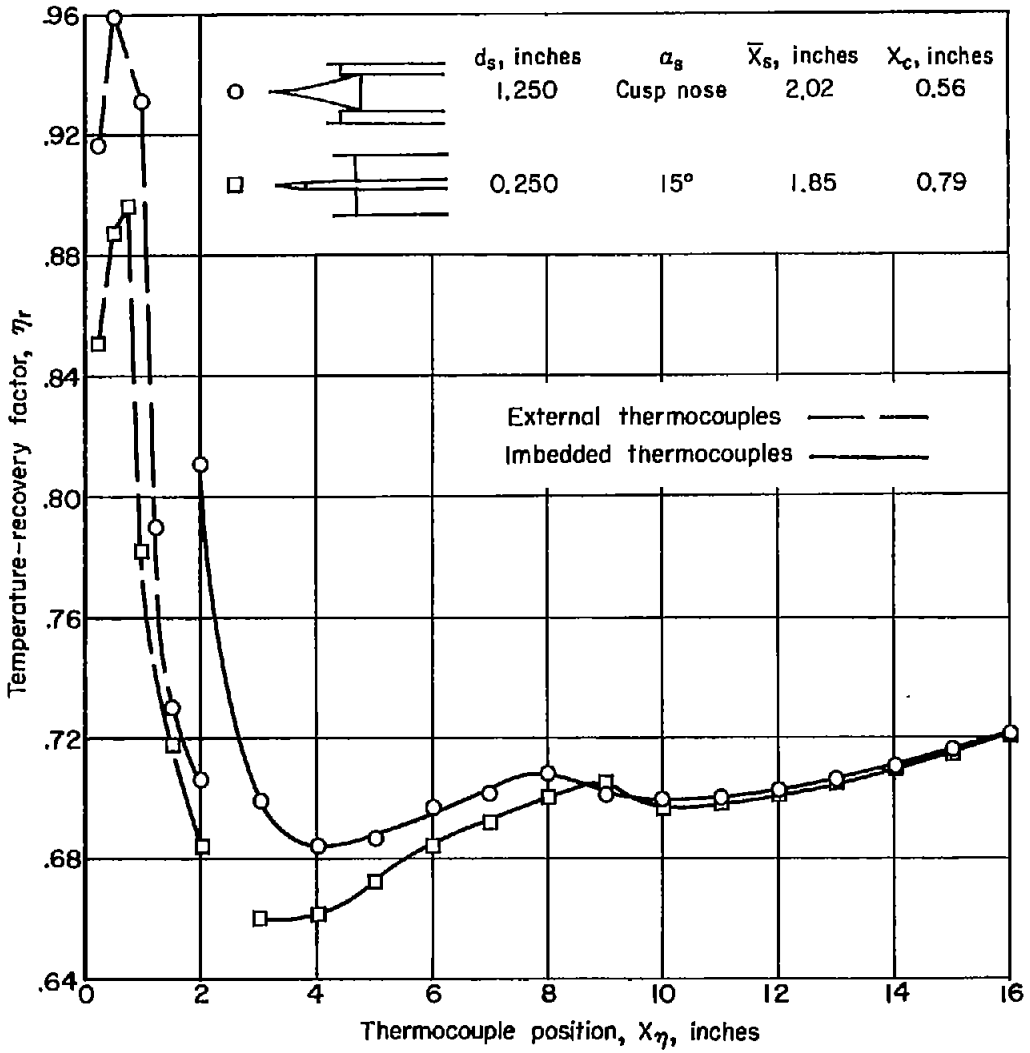

Figure 9.- Comparison of recovery factor along the cylinder for two spikes.

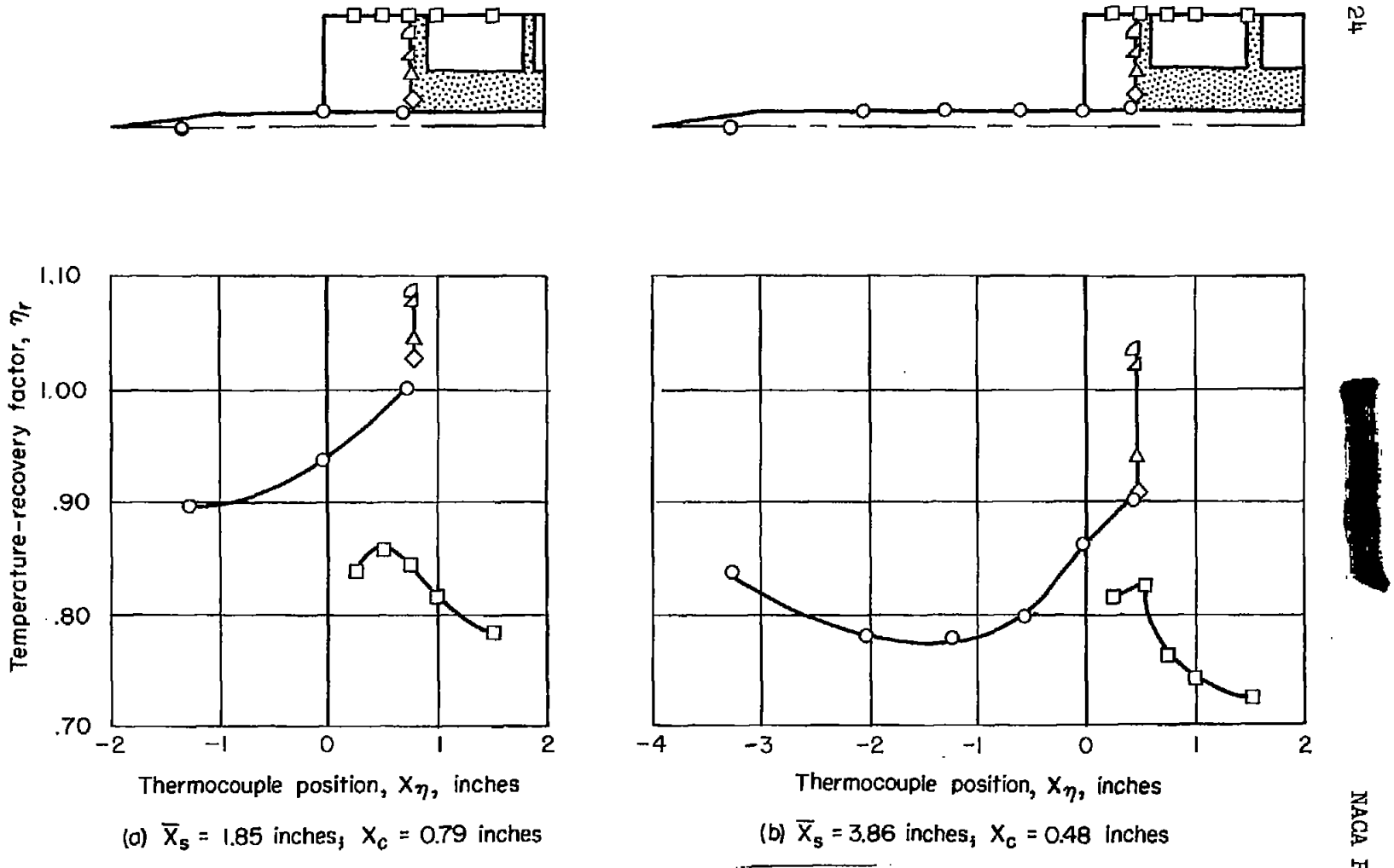

(a) $\overline{X}_s$ = 1.85 inches; X_c = 0.79 inches

(b) $\overline{X}_s$ = 3.86 inches; X_c = 0.48 inches

Figure 10.- Recovery factors in the spike-nose region; d_s = 0.250 inch, α_s = 15°.

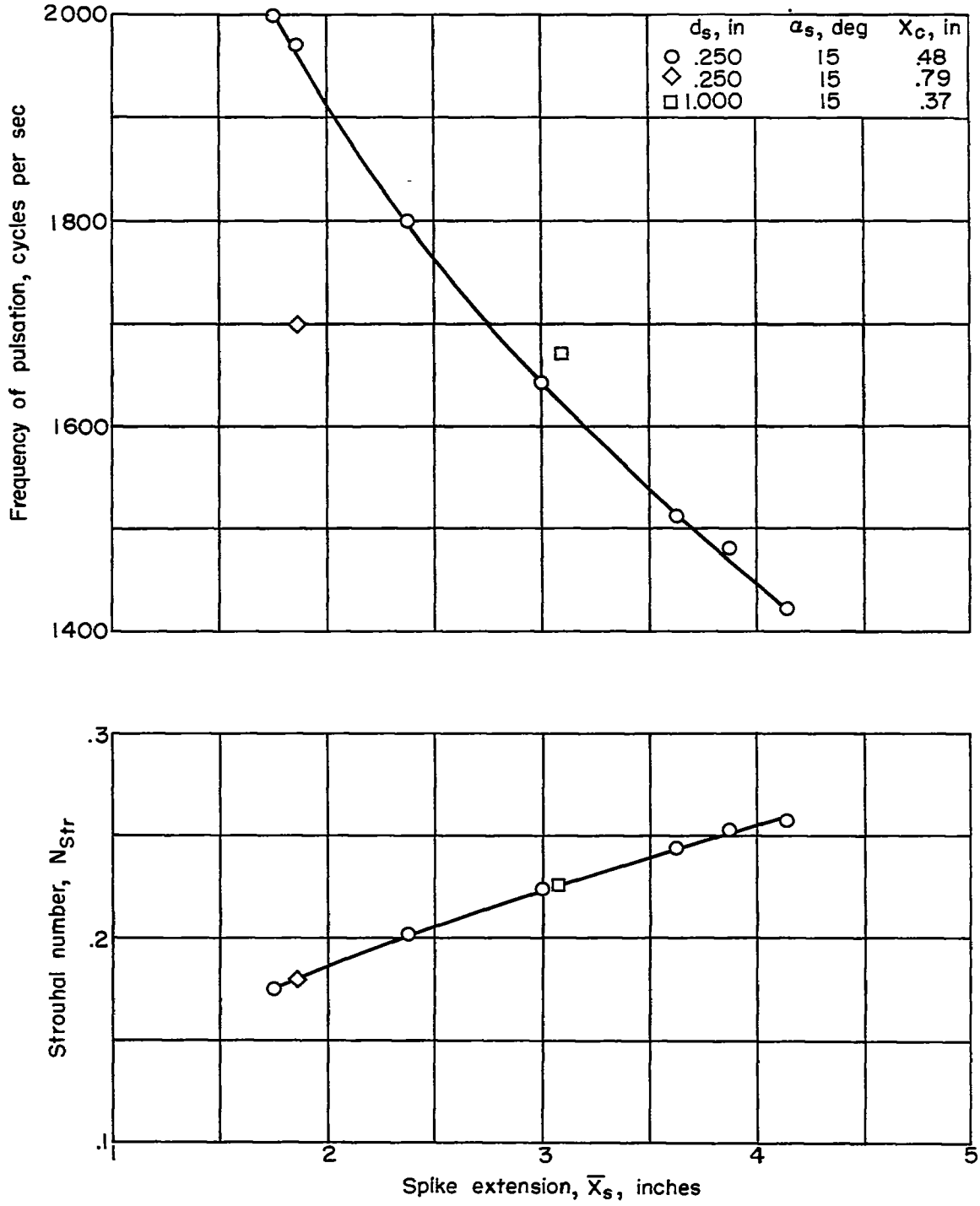

Figure 11.- Variation of frequency and Strouhal number with spike extension.

[redacted]